Dispersion of silicon carbide nanoparticles in a AA2024 aluminum alloy by a high-energy ball mill

C. Carreño-Gallardo, I. Estrada-Guel, C. López-Meléndez, **R. Martínez-Sánchez**

Abstract

Al2024 alloy was reinforced with silicon carbide nanoparticles (SiCNP), whose concentration was varied in the range from 0 to 5 wt.%; some composites were synthesized with the mechanical milling (MM) process. Structure and microstructure of the consolidated samples were studied by X-ray diffraction and transmission electron microscopy, while mechanical properties were investigated by compressive tests and hardness measurements. The microstructural evidence shows that SiCNP were homogeneously dispersed into the Al2024 alloy using high-energy MM after 2 h of processing. On the other hand, an increase of the mechanical properties (yield stress, maximum strength and hardness) was observed in the synthesized composites as a direct function of the SiCNP content. In this research several strengthening mechanisms were observed, but the main was the obstruction of dislocations movement by the addition of SiCNP.

Keywords

Aluminum alloy; SiC; Mechanical alloying; Composites

1. Introduction

Particle-reinforced metal matrix composites (MMCs) exhibit improved mechanical and physical properties which combine the advantages of both the matrix and the reinforcing materials. Although various metals have been studied as matrix materials, aluminum alloys have been used as the matrix materials in most of

the particle-reinforced MMCs in the industry [1]. Discontinuously Reinforced Aluminum materials are produced usually by sintering process. This step includes the homogenization of microstructure and improves the composite densification [2].

Some research has been focused on the synthesis and application of metal matrix composites (MMCs) in recent years. Metal and ceramic particles have mainly been used as reinforcing materials. Aluminum and its alloys have been reinforced with ceramics in order to improve properties like wear behavior or mechanical strength [3]. However, most of them are related to the use of micron sized particles [4].

These materials are manufactured by means of atomized pure powder or alloyed powder, mixed with ceramic powders and processed by mechanical alloying (MA), followed by die compaction, hot extrusion and heat treatments. Final properties of the metal matrix composites (MMCs) depend on many factors: the matrix and the ceramic materials properties, bond between ceramic and matrix, and size and distribution of the ceramic into the metallic matrix. Therefore, MA offers a decrease in the ceramic size during milling and a lower risk of segregation and the ceramic nanoparticles agglomeration. A better homogeneity of the ceramics into the metal matrix is achieved by MA [5].

Micron-sized particles are commonly used to improve the ultimate tensile and the yield strengths of the metal matrix [4]. However, this has a counterpart, since the ductility of the MMCs significantly decreases as the concentration of ceramic particles is increased. It results very interesting to use nano-sized ceramic particles due to the fact that they strengthen the metal matrix but keeping a good ductility.

The mechanical properties of these compounds are not only significantly influenced by the quantity and way of distribution of the reinforcing materials, but also by the nature of the interface between the reinforcement and the matrix, as well as by the possible strengthening mechanisms working due to a heat treatment.

The mechanical milling is considered as a promising and commercial technique because it ensures a homogeneous distribution of both, the alloying elements and the reinforcement materials [6]; [7]; [8] ; [9]. Thus, aluminum-matrix composites have been successfully used in aircraft, automobile and other means of transportation such as engine pistons, brake drums and electronic packaging. Further application is expected with the development of low-cost processing methods. However, the effect size of reinforcement phases is still under research, as well as the strengthening mechanisms working in the composite materials.

This work is focused on the dispersion of SiCNP by a milling process, and on the study of nanoparticles effects on the mechanical properties and microstructural evolution during T6 temper in Aluminum based composites.

2. Experimental procedure

Aluminum alloy AA2024 (Al–4.00% Cu–0.83% Mg–0.21% Fe–0.67% Mn–0.12% Si–0.03% Cr) was used as a matrix of composites and silicon carbide nanoparticles (SiCNP) as reinforcement. SiCNP were dispersed into the aluminum matrix to form nanocomposites by a milling process. AA2024 was received as a metal bar, where debris, were obtained by drilling it. Table 1 shows the percentages of SiCNP and the milling times used in this research.

Table 1
Concentration of SiC_{NP} and milling time.

Matrix	Milling time (h)	Reinforcement agent	Concentration (wt.%)				
AA2024	2	SiC_{NP}	0.0	0.5	1.5	2.5	5.0
	5	SiC_{NP}	0.0	0.5	1.5	2.5	5.0

The milling processes were done with an energy ball mill SPEX 8000M. Milling times were 2 and 5 h, based on previous works [10] ; [11]. The mass of the powders was of 8.5 g and a ball-to-powder weight ratio was 5:1. 10 drops of methanol were used as a process control agent (PCA) in all milling experimental tests. Argon was used as an inert atmosphere during milling to avoid excessive metal oxidation. Milling products were cold consolidated at 330 MPa by a cylindrical steel die (compacting device) in order to obtain samples with 5 mm of diameter and 10 mm high. Green products were pressure-less sintered for 3 h at 500 °C under an argon atmosphere. An unreinforced alloy was prepared by the same route for a comparative purpose.

After sintering, the specimens were thermically treated using a heat treated solution for 1 h at 495 °C and quenching in room temperature water. Then, samples were artificially aged (T6 Temper) for 12 h at 191 °C. After heat treatment, products were characterized by X-ray diffraction (XRD) in a PANanalytical XPert Pro diffractometer, with Cu Kα radiation (λ = 1.5406 Å), operated at 40 kV and 25 mA, in the 2θ range of 20–90°. The Step and the collection time were 0.05° and 5 s respectively. The nanoparticle sizes and distribution, and the morphology and microstructure of the composites were determined by transmission electron microscopy (TEM) by using a JEOL-EM 2200FS microscope operating at 200 kV. The hardness measurements were done on compacted sample surfaces by using

Rockwell scale F (HRF) with a load of 60 kg. The cylindrical shaped compression specimens were tested by using the compressive test with a constant strain rate of 10−3 s−1. The yield strength (σy) and maximum strength (σmax) were determined with the after mentioned compression test in an Instron model 3382 not important testing machine. The average of three measurements was registered and reported. σmax was determined arbitrary at 0.1 of deformation and the yield stress was determined at the 0.2 pct offset.

3. Results and discussion

Fig. 1 shows an image from TEM of SiCNP. It is noticeable their facet-based morphology and the size lower than 100 nm. The inset box shows a zoom view of SiCNP, and the zones where the EDS microanalyses were done. From microanalysis of SiCNP, an atomic relationship very close to an equiatomic ratio was found.

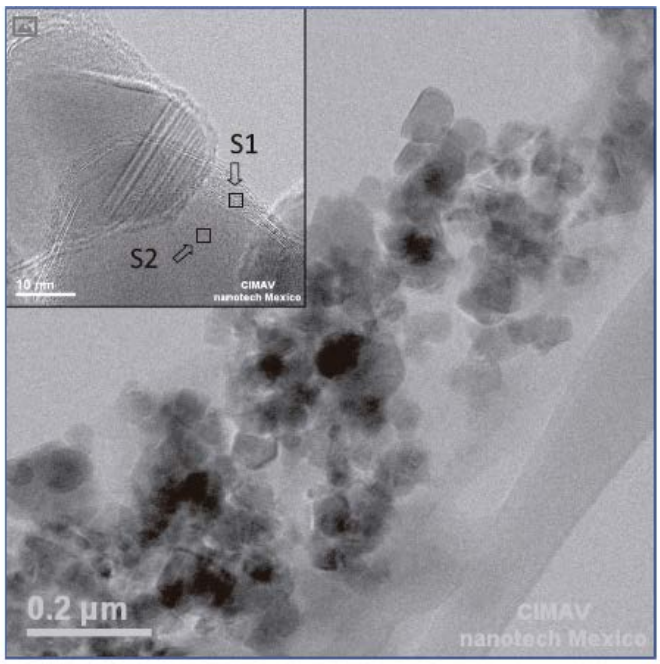

Fig. 1. Morphology and size of the SiC_{NP} used as reinforcement material.

XRD patterns of the AA2024 and their composites are shown in Fig. 2. This figure shows the patterns of samples in different conditions such as milled, sintered at 500 °C and heat-treated by T6. Fig. 2a shows the results for 2 h of milling and Fig. 2b for 5 h of milling as well. There is a difference of 2 at the principal peaks of the Al in between Fig. 2a and b. The XRD pattern of sample in green condition (as-milled) not only shows the characteristic peaks of aluminum but also the ones belonging to the silicon carbide nanoparticles after 2 h of milling. From measurements at different milling times (2 and 5 h) it was observed that the aluminum peaks show a small shift to the left, which could indicate a lattice parameter growth, due to the formation of the solid solution. The peaks belonging to the NP show small intensities which are in agreement with the nanoparticles concentration.

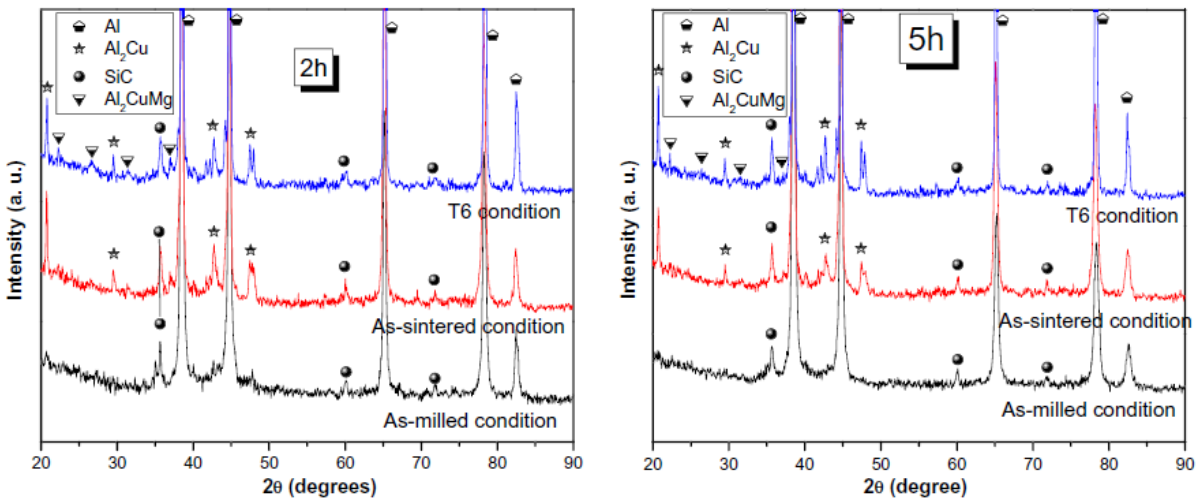

Fig. 2. XRD patterns of as-milled condition, as-sintered and T6 condition samples at different milling times, (a) 2 h and (b) 5 h.

The XRD pattern for the sintered sample illustrates a refinement in the signals of the aluminum solid solution. It also shows the presence of signals involving the balance related to Al2Cu (θ) phase. It is expected that this phase is formed inside the solid solution, which is started during the milling process, due to the diffusion mechanisms favored by the temperature and the time of sintering [12]. The nanoparticle peaks have no significant changes, because of their high stability into the aluminum matrix.

The presence of a new phase in the XRD pattern is observed after the T6 heat treatment which corresponds to the variation upon the phase (θ), which was identified as Al2CuMg. This phase and also Al2Cu is formed during the T6 heat treatment. Similar outcomes were found with samples that were milled for 5 h. Only a slight decrease was observed in the intensity of the peaks when the milling time increased, which would be associated to the increase of the plastic strain of the powders, which is a common effect on samples which are submitted to mechanical high energy milling process [13].

4. Hardness measurement

Fig. 3 shows the hardness values obtained in the HRF scale for the composites in the T6 condition synthesized in different milling times. Fig. 3a and b shows the results for 2 h and 5 h of a milling process respectively. The reported hardness values in the literature for a commercial alloy 2024-O are included in both Fig. 3a and b. It is noticeable that the synthesized composites show better properties than the commercial alloy. These figures show that the lower the milling

times the better the results. There is a significant difference between both milling times due to the low compressibility that the milled materials performed during a longer time (5 h). Fig. 3b shows the behavior of hardness for 5 h of milling time. The hardness of composite containing 0.5 wt.%. SiCNP is lower than that of sample with no additions of SiCNP. This could be attributed to an excessive hardening by strain (5 h of milling time), responsible for a poor densification during the consolidation process.

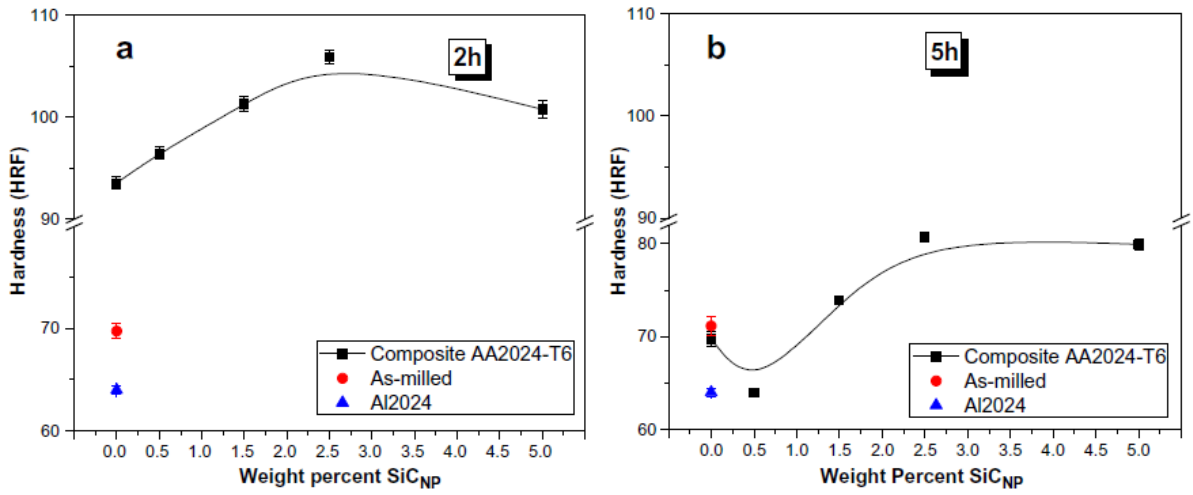

Fig. 3. Hardness variation average values vs SiC_{NP} weight percentage at different milling times: (a) 2 h and (b) 5 h.

For 2 h of milling there is a direct relationship between the hardness and the content of the SiC nanoparticles. There is an appreciable hardness saturation value of 105.76 HRF at 2.5% SiCNP concentration. At higher NP concentrations only a slight decrease in the hardness values was observed. In Fig. 3a is clear the obtained reinforcing effect from the nanoparticles and the effect of the milling process in the mechanical properties of the alloy 2024-O. However, it is impossible to put away the effect that the nanoparticles might have on the sequence of precipitation during the registered T6 treatment [13].

Regarded to samples with 0.0% of SiCNP, it is observed that the milled

samples present a hardness 5 unit bigger than the Al2024 samples reported in the literature. Upon condition T6, the hardness increment is much bigger. This increment after the T6 temper is mainly due to the Al2Cu and Al2CuMg precipitation phases.

5. Compression test

Fig. 4 shows the obtained values for the yield strength (σy) and the maximum strength (σmax). The values from the samples are placed in the same figure with T6 condition and 2 h of milling process. Literature values [14] from the alloy 2024 were compared in two conditions; annealed and T6 with the purpose of clarification of effects. Fig. 4a shows the obtained results for the σy. It is observed that, as in the case of hardness with the same synthesis conditions, there is a clear influence of the nanoparticle content on the σybehavior, up to a saturation value of about 450 MPa.

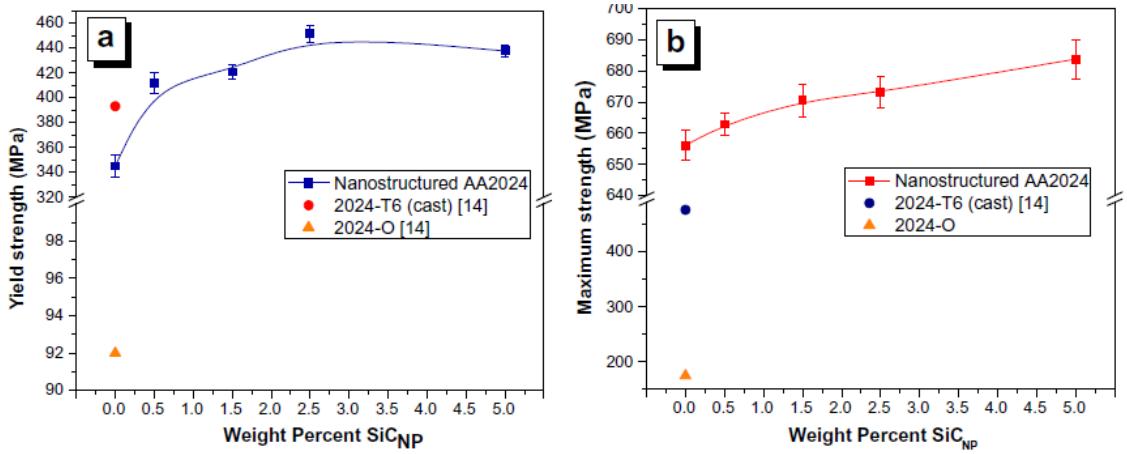

Fig. 4. Yield strength (a) and maximum strength (b) as a function of SiC_{NP} content in 2 h milled composites. Reported values from 2024-O and 2024-T6 commercial alloys are also included.

The saturation point for the σy and the hardness match up in 2.5 wt.% NP. The reported values for commercial alloy by using the T6 condition are slightly greater than those achieved in the alloy without reinforcement. This is due to the porosity found in the sintered samples [15], in which there is a considerably

decrease of the mechanical resistance during the compression test. However, the compression values of the reinforced alloys are still significantly important and should be taken into account.

Fig. 4b shows the results of σmax. A direct relationship between σmax and SiCNP content can be observed. Data dispersion is a little lower than in the case of σy. No saturation point, as in the case of hardness and σy, can be observed at 2.5 wt.% SiCNP. Though, an important decrement in ductility in the composites with 5 wt.% NP was observed. The porosity effect on σmax is not perceptible because all of the values observed in the samples are higher than the ones reported for the commercial alloy 2024.

Similar behavior on mechanical properties in aluminum based composites was reported by Yang et al. [16]. Final values found for σmax and σy, which are attributed to the nano-sized ceramic particles and mechanical milling process, show a significant increment. Even in aluminum based composites reinforced with ductile nanoparticles, the values reported for σmax and σy are higher compared with the unmodified alloy [10] ; [11].

Almost linear increment of mechanical properties as a function of the content of the SiC nanoparticles might be due to several strengthening mechanisms such as nanoparticle hardening by dispersion, interaction of NP with dislocation lines, mismatch because of differences in thermal expansion, and possible anchorage of grain boundaries which prevents its growth [17]. Fig. 5 shows TEM micrographs of the composite after T6 treatment. Fig. 5a illustrates SiC the homogeneous dispersion into the aluminum matrix (indicated with white arrows on the micrograph);

however, although the observed area is too small, the micrograph is a good example of the whole area analyzed during the characterization throughout TEM studies. Fig. 5b shows a TEM micrograph of an area where grain boundaries can be seen. TEM micrograph shows the presence of SiCNPtrapped into a grain boundary. Nevertheless, the small amount of particles into the grain limits cannot account for the grain boundary anchorage.

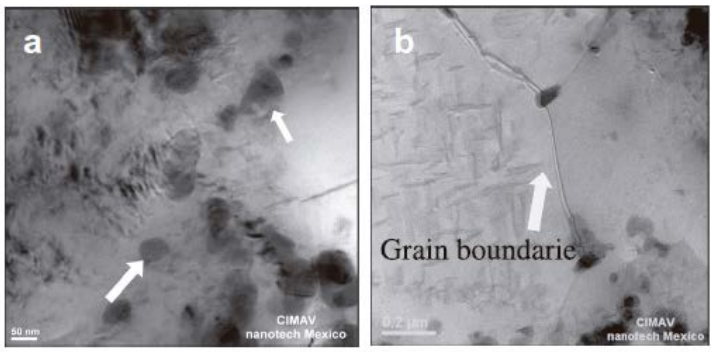

Fig. 5. Distribution of SiC_{NP} in AA2024 matrix (a), and SiC_{NP} on grain boundaries (b).

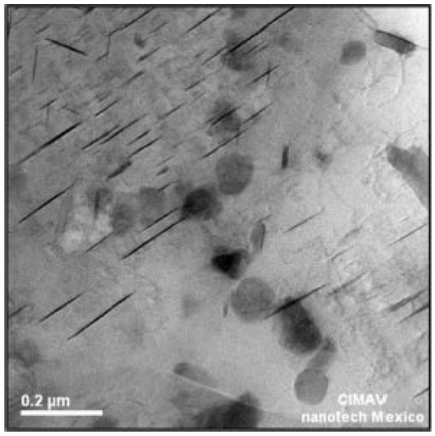

Fig. 6. TEM micrograph showing the coexistence of precipitates with SiC_{NP}.

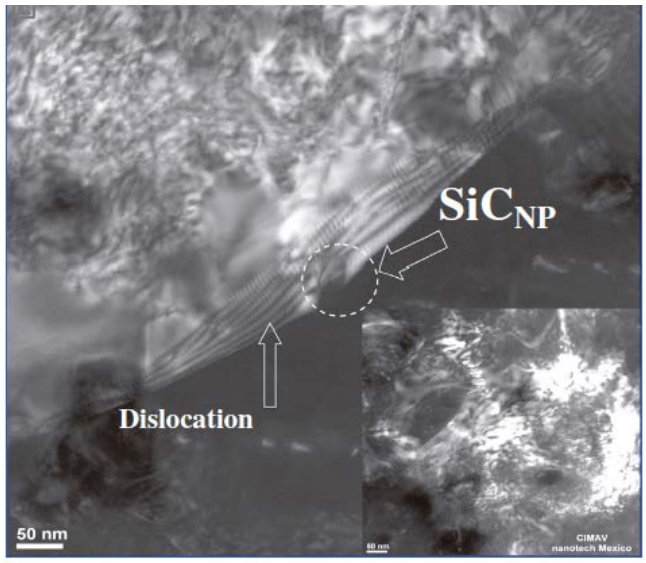

Fig. 7. Interaction of dislocation lines with SiC_{NP}.

Believed that the properties of MMCs would be enhanced consider-ably even with a very low volume fraction due to the high disloca-tion density of metal matrix.

Fig. 6 shows the coexistence of the precipitates formed during the T6 treatment with the SiCNP. Fig. 7 provides evidence of the interaction between the dislocation lines and the nanoparticles, which might be the starting point of the mechanism reported by Orowan [19] even though the particle looping by the dislocation line is not clearly observed.

6. Conclusions

SiC nanoparticles can be uniformly incorporated into AA2024 matrix by a milling process. Consolidated materials were synthesized by conventional powders metallurgy route. Hardness, yield strength and compressive strength of

nanostructured AA2024 composites increased with increasing SiCNP content. Short milling times (2 h) gave the best response on the mechanical properties of composites. Several mechanisms were hypothesized which contribute to the strengthening of the alloys.

Acknowledgements

This research was supported by CONACYT (106658). Thanks to Redes Temáticas de Nanotecnología y Nanociencias Regs. 0124623 and 0152992. The authors gratefully acknowledge the efforts of D. Lardizabal-Gutierrez, W. Antúnez-Flores, J.E. Ledezma-Sillas, E. Torres-Moye, R. Castañeda-Balderas, and C. Ornelas-Gutierrez for their technical assistance.

References

[1] W.H. Hunt, in: T.W. Clyne (Ed.), Comprehensive Composite Materials, Metal Matrix Composites, vol. 3, Elsevier Ltd., 2003, pp. 701–715.

[2] C. Suryanarayana, Prog. Mater. Sci. 46 (2001) 1–184.

[3] C.L. De Castro, B.S. Mitchell, Mater. Sci. Eng. A 396 (2005) 124–128.

[4] K.M. Mussert, W.P. Vellinga, A. Bakker, S. Van Der Zwaag, Mater. Sci. 37 (2002) 789–794.

[5] C.E. Da Costa, W. Zapata, J.M. Torralba, J.M. Ruiz-Prieto, V. Amigó, P/M MMCs base aluminium reinforced with Ni3Al intermetallics made by mechanical alloying route, in: Materials Science Forum, vol. 21, Trans. Technol. Publications, Suiza, 1996, pp. 1859–1864.

[6] H. Lagace´ , D.J. Lloyd, Metall. Quart. 28 (1989) 145–152.

[7] P.L. Liu, Z.G. Wang, W.L. Wang, Mater. Sci. Technol. 13 (1997) 667–

672.

[8] Y.B. Liu, J.K.M. Kwok, S.C. Lim, L. Lu, M.O. Lai, J. Mater. Proc. Technol. 37 (1993) 441–451.

[9] NP Suh (Ed.), Tribophysics, Prentice-Hall, 1986.

[10] R. Martínez-Sánchez, J. Reyes-Gasga, R. Caudillo, D.I. García-Gutiérrez, A. Márquez-Lucero, I. Estrada-Guel, D.C. Mendoza-Ruiz, M. José Yacaman, J. Alloys Comp. 438 (2007) 195–201.

[11] C. Carreño-Gallardo, I. Estrada-Guel, M.A. Neri, E. Rocha-Rangel, M. Romero-Romo, C. López-Meléndez, R. Martínez-Sánchez, J. Alloys Comp. 483 (1–2)(2009) 355–358.

[12] M. Aravind, P. Yu, M.Y. Yau, Mater. Sci. Eng., A 380 (2004) 384–393.

[13] R. Pérez-Bustamante, M.J. González-Ibarra, J. González-Cantú, I. Estrada-Guel,

J. M. Herrera-Ramírez, M. Miki-Yoshida, R. Martínez-Sánchez, J. Alloys Comp. 536S (2012) S17–S20.

[14] ASM Handbook, in: 10th (Ed.), Properties and selection: Nonferrous alloys and special-purpose materials, vol. 2, ASM International, 1997.

[15] Liang Xue, Tomasz Wierzbicki, Int. J. Appl. Mech. 1 (2) (2009) 267–304.

[16] Y. Yang, J. Lan, X. Li, Mater. Sci. Eng. A 380 (2004) 378–383.

[17] M.H. Enayati, M.R. Bafandeh, S. Nosohian, J. Mater. Sci. 42 (2007) 2844–2848.

[18] R.J. Arsenault, Sci. Eng. 64 (1984) 171–181.

[19] R. Dieter, Mechanical Metallurgy, 3rd., McGraw-Hill, New York, 1986.